On-line polymerisation monitoring in $scCO_2$: a reliable and inexpensive sampling method in high pressure applications

Kristoffer Kortsen[a], Ana A.C. Pacheco[a], Joachim C Lentz[a], Vincenzo Taresco[a], Steven M. Howdle[a,*]

[a] University of Nottingham, School of Chemistry, University Park, NG7 2RD, UK

[*] Corresponding author. E-mail address: steve.howdle@Nottingham.ac.uk

Keywords

Supercritical CO_2 ; On-line monitoring ; Sampling ; Kinetics ; Polymerisations

Abstract

A versatile and reliable on-line sampling system for polymerisation reactions in supercritical fluids was developed. By withdrawing a small volume of a high-pressure reaction mixture and expanding it in a controlled volume, reliable kinetic data was obtained for a range of reactions in scCO2, avoiding the need for costly equipment or setup modifications. All experiments were carried out in a stainless-steel high-pressure autoclave with mechanical stirring and a volume of 60 ml. With the polymerisation of methyl methacrylate (MMA) in scCO2 being widely adopted for research in the past, the free-radical and RAFT controlled dispersion polymerisations of MMA were analysed in detail using the sampling system as a proof-of-concept. Additionally, initial implementation of the sampling system to a range of different reactions showed the facile applicability of the monitoring method.

1. Introduction

Current industrial polymer particle production processes often use water as the main solvent, generally resulting in contamination of that water through the use of volatile organic compounds (VOCs) and chlorofluorocarbons (CFCs)[1, 2]. This results in contaminated wastewater streams, with negative consequences for the environment, oceans and availability of drinking water. Additionally, water must be removed from the final product, in costly and energy intensive drying processes, further increasing the negative environmental impact[2, 3]. As environmental impact

becomes a more pressing concern, there is an increasing interest in alternative solvents that have the potential to alleviate water contamination issues, reduce energy costs and reduce the impact on the environment[4].

Supercritical carbon dioxide ($scCO_2$) is a promising alternative solvent, combining considerable environmental advantages[5] with the desired solvation and diffusivity properties of SCFs[3, 6-8]. It is a cheap, non-flammable and environmentally friendly solvent[5], with an easily attainable critical point at relatively mild conditions (T_c = 31.1 °C and P_c = 73.8 bar)[3, 8]. A further advantage of using $scCO_2$ as a polymerisation medium, is found after the reaction is complete. When returning to atmospheric conditions, CO_2 reverts to the gas phase providing a solvent free polymer product, without the need for energy and cost intensive drying processes.

The poor solubility of most common high molecular weight polymers in $scCO_2$, makes it an ideal continuous phase for heterogeneous polymerisations[3, 8, 9]. Most common and industrially important vinyl monomers, (e.g. methyl methacrylate (MMA)), are highly soluble in $scCO_2$, while the corresponding polymers are poorly soluble[3, 8-10]. MMA has been an essential monomer for research, being used for the first precipitation polymerisations in $scCO_2$, with molecular weight being controlled through the use of a chain transfer agent (CTA)[3]. The respective CO_2-philicity and CO_2-phobicity of MMA and PMMA was again exploited for the first dispersion polymerisation conducted in $scCO_2$[11]. Research into stabilisation methods for dispersion polymerisations continued to employ MMA as the model monomer of choice to expand fundamental understanding[3, 5, 6, 12-17]. Reversible-deactivation radical polymerisation (RDRP) has also been thoroughly investigated in $scCO_2$[18], with successful implementation of nitroxide mediated polymerisation (NMP)[19, 20], atom transfer radical polymerisation (ATRP)[21] and reversible addition-fragmentation chain-transfer (RAFT) [22-24]. While NMP research relied on styrene, MMA was used extensively as the reference monomer for ATRP and RAFT polymerisation in $scCO_2$.

The determination of kinetic behaviour of a polymerisation reaction relies on two essential factors. Firstly, it requires a complete description of reactions occurring in the system during polymerisation. Secondly, it requires a reliable method of measurement, allowing the reaction progress to be tracked throughout. Thorough descriptive models have been developed for a range of polymerisations in $scCO_2$ – again relying on MMA as the model monomer – allowing for detailed fittings of experimental data that can be gathered[25-29]. However, a reliable and accessible monitoring method is still required if $scCO_2$ reaction systems are to be implemented more readily throughout research and industry.

The tracking of an ongoing polymerisation reaction in traditional solvents can be achieved with a wide range of techniques[30]. Reactions in $scCO_2$ however, are more complicated to monitor due to the elevated pressure present in sealed systems. Spectroscopic techniques can be used in $scCO_2$, but require bespoke and specialised equipment, capable of withstanding the high system pressures and because of this the use of on-line spectroscopic techniques for polymerisations in $scCO_2$ is currently limited.

FTIR has been used to monitor the precipitation polymerisation of acrylic acid in $scCO_2$[31]. While the viability of the technique was confirmed by comparing polymerisation results in $scCO_2$ to the atmospheric polymerisation in toluene and model fittings, the widespread use of IR in $scCO_2$ is hampered by the costly and precise setup required.

Turbidimetry, unlike static or dynamic light scattering[32, 33], is not sensitive to multiple scattering disruptions and can therefore be used for the monitoring of strongly scattering suspensions as found in $scCO_2$ polymerisations[34]. While this can provide on-line polymerisation monitoring, It does require costly apparatus to allow line-of-sight through the reaction medium[35-38].

Raman spectroscopy, another technique used widely for on-line monitoring of polymerisations[39], has also been implemented in $scCO_2$ reaction monitoring[40]. As with IR spectroscopy and turbidimetry, Raman spectroscopy requires the incorporation of a window into the body of the reactor for incident light interaction with the reaction medium. While Raman spectra can be captured at location of the incident light, avoiding the need for a fixed path length or second window[41], the overall cost of such a setup forms a barrier to widespread implementation.

An on-line monitoring technique that does not require the incorporation of windows or probes into the reactor setup is power compensation calorimetry[42-45]. Polymerisation progress can be tracked by monitoring the power required to maintain system temperature at the desired level. When the exothermic polymerisation reaction occurs, less power will be needed to maintain reactor temperature and power output can then be correlated to polymerisation progress. Despite the accurate data this method can provide, the efficacy is very dependent on the thermal properties of the reaction and does not easily provide molecular data. The setup is also scale sensitive, as calorimetry is generally not applicable to large scale systems.

Polymerisation reactions at atmospheric pressure are easily monitored by sampling a known volume from the reactor at regular intervals. This volume can then be analysed for polymer content, conversion and/or molecular weight averages[39]. This technique can also be applied to polymerisations in $scCO_2$, but the reaction setup must be modified to allow for this. The autoclave requires a needle valve exit to allow for sampling, as described by Thurecht and co-

workers[46]. Polymer conversion can then be followed via ^{1}H NMR measurement, comparing the polymer concentration to residual monomer concentration[6]. While simply collecting a sample from a needle valve exit can provide a reliable sample, the major problem is that volatile components will be lost, resulting in erroneous results. Additionally, the method of sample collection introduces sharp pressure fluctuations, that can have a detrimental impact on the ongoing reaction.

The goal of the research presented here was to develop a reliable and widely applicable sampling method applicable to supercritical fluid reaction, and that could be directly comparable to online monitoring techniques used for atmospheric polymerisations throughout research and industrially[30, 47-49]. The system was developed to be simple, reliable and inexpensive. After developing a viable sampling method, the system was tested using MMA as a proof-of-concept monomer. Further to this, a range of initial tests were conducted to show the ease of application of the novel method to a range of different types of reactions.

2. Materials and methods

2.1. Chemicals used

Methyl methacrylate (MMA, 99 %) was obtained from Mitsubishi Chemical. 2,2'-Azobis(isobutyronitrile) (AIBN, 98 %) was purchased from Molekula. Methacrylate terminated polydimethylsiloxane (PDMS-MA, 150-200 cSt) was acquired from Fluorochem. 2-cyano-2-propyl dodecyl trithiocarbonate (CPDT, 97 %), Styrene (99 %), acrylic acid (AA, 99 %) and 2-Hydroxyethyl methacrylate (HEMA, 97 %) were purchased from Sigma-Aldrich. ε-Caprolactone (CL, 99 %) was obtained from Fisher Scientific. Novozym-435 (Candida Antarctica lipase B immobilized on acrylic resin) was kindly donated by Novozymes A/S, Denmark. Carbon dioxide (CO_2, SCF grade 5.5, 99.9995 %) was obtained from Air Products and Chemicals Inc. Unless explicitly stated, all chemicals were used as received.

2.2. Reactor setup and sampling procedure

Traditional batch type experiments were carried out using an in-house built high-pressure reaction vessel with an internal volume of 60 ml (max. operating conditions: 120 °C, 380 bar), detailed in previous publications[6, 46, 50, 51]. Successive reactions were halted by submerging the system in an ice water bath, cooling the system to subcritical temperatures within a minute. The pressure was then released, and the product was analysed for conversion and molecular weight, in line with the methodology used across the research field previously[10, 17, 28, 52, 53]. This was done to establish a reference baseline for expected conversion values.

On-line monitoring experiments were carried out using a similar setup, with an additional needle valve exit controlled by a sampling outlet tap (*Fig. 1*). This outlet is connected to a 150 ml stainless-steel cylinder via 7 cm of 1/8-inch tubing (internal volume of 0.18 cm^3) and a needle valve tap, all purchased from Swagelok (*Fig. 2*). The double ended cylinder is capped by a bonnet tap with integrated burst disk on the far end. The autoclave is put upon a pedestal with a hole to allow access to the additional exit in the base of the autoclave.

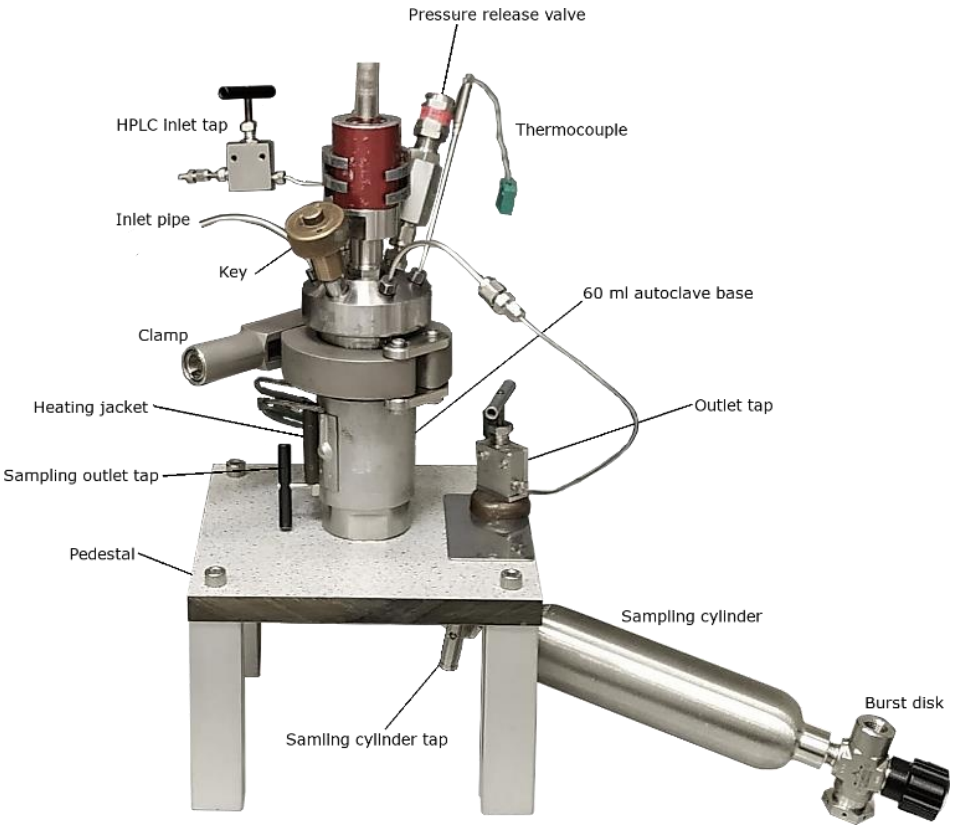

Fig. 1. *60 ml high pressure autoclave setup used for monitoring experiments.*

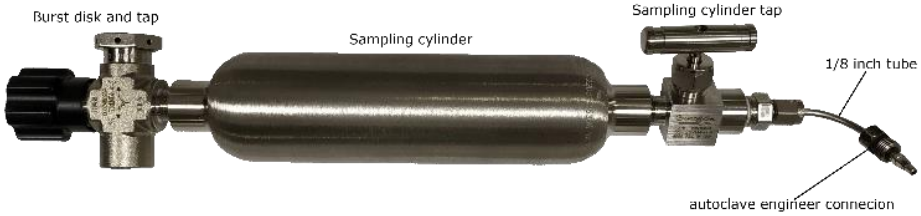

Fig. 2. *Cylinder system used to obtain on-line samples during monitoring experiments. Swagelok product codes: burst disk and tap: SS-16DKM4F4-A-2, sampling cylinder: 36L-50DF4-150-T, sampling cylinder tap: SS-20VM4-F4*

Prior to on-line sampling, the sampling cylinder was loaded with 5 ml of a deuterated solvent. If required, an internal standard can be added to the solvent. A deuterated solvent was used so that the obtained mixture could be analysed directly by NMR, but basic lab solvents can also be used. The cylinder system was then attached to the sampling outlet

using the Autoclave Engineer connection. With all taps closed firmly, CO_2 was added to the autoclave to increase the internal pressure by 15 bar. The sampling outlet tap was then opened, filling the 1/8-inch tube with approximately 0.18 ml of autoclave content and causing the pressure to drop by 15 bar. After closing the sampling outlet tap, the sampling cylinder tap was opened. The contents of the high pressure 1/8-inch tube releases directly into the cylinder chamber, where it is captured into the deuterated solvent. The cylinder system was then detached from the autoclave and the sample – dissolved in the chosen deuterated solvent – was recovered by pouring the content back through the 1/8-inch tube into a glass vial. The recovered solution was analysed for conversion and molecular weight. The cylinder system was rinsed with a good solvent for the polymerisation product and dried before repeating the procedure to obtain the next sample. A cylinder volume of 150 ml was chosen to allow for the capture of a high-pressure sample while keeping the final cylinder pressure below 2 bar.

2.3. Analysis techniques

2.3.1. NMR

The conversion of each obtained sample was determined using ^{1}H nuclear magnetic resonance spectroscopy (^{1}H NMR). Samples were dissolved in a suitable deuterated solvent ($CDCl_3$, D_2O or DMSO-d_6) and analysed using a Bruker DPX 400 MHz spectrometer. Chemical shifts were assigned in parts per million (ppm). All spectra were obtained at ambient temperature (22 ± 1 °C). MestReNova 14.0.1 copyright 2019 (Mestrelab Research S.L.) was used for analysing all spectra.

2.3.2. GPC

Gel permeation chromatography (GPC) was performed with THF (HPLC grade, Fisher Scientific) as the eluent at room temperature using two Agilent PL-gel mixed-C columns in series with a flow rate of 1 ml min^{-1}. Sample detection was achieved using a multiangle light scattering detector and differential refractometer. The system was calibrated using narrow dispersity PMMA standards.

2.3.3. SEM

Scanning electron microscopy (SEM) was used to image formed polymer particles. Polymer powder samples were mounted on SEM stubs using carbon tape. To avoid charge build-up in the sample, a platinum coating was applied to the samples prior to SEM imaging. The coated particle samples were then imaged using a FEI Phillips XL30 SEM. The

image analysis software Fiji(ImageJ) was used to determine the number average particle diameter (d_n) by measuring 100 particles from obtained images.

2.4. Free-radical dispersion polymerisation of MMA

All reactions were conducted with MMA (9.36 g, 10 ml), PDMS-MA stabiliser (5 wt% relative to MMA, 0.468 g) and AIBN initiator (0.25-2 wt% relative to MMA, 23.4-187.2 mg) in a 60 ml high pressure autoclave. MMA, PDMS-MA and AIBN were all degassed by bubbling with argon in separate vials for 30 minutes. During this time, the autoclave was flushed with CO_2 at 2-3 bar, venting through the keyhole (*Fig. 1*). After 30 minutes, MMA (7.5 ml, 7.02 g) was added to the PDMS-MA vial and this mixture was injected into the autoclave through the keyhole against a positive flow of CO_2. The key was then inserted into the autoclave, sealing it off from the atmosphere. At this point CO_2 was added, pressuring the system to 50 bar. Heat was then applied through the heating jacket, bringing the temperature to 65 °C. CO_2 was then added until the system pressure reached 200 bar. The AIBN initiator was added to the autoclave along with MMA (2.5 ml, 2.34 g) using a JASCO LC-4000 HPLC pump at a flow rate of 1 ml/min. The pressure was then raised to 220 bar by adding CO_2, if needed. The end of the initiator injection was chosen as the starting point of the reaction.

2.5. RAFT controlled dispersion polymerisation of MMA

The reaction was conducted with MMA (0.1 mol, 10 g), PDMS-MA stabiliser (5 wt% relative to MMA, 0.5 g) and AIBN initiator (0.085 mmol) and the chain transfer agent 2-cyano-2-propyl dodecyl trithiocarbonate (CPDT) (0.17 mmol) in a 60 ml high pressure autoclave. All reagents were kept on ice and degassed by bubbling with argon for 30 minutes. During this time, the autoclave was flushed with CO_2 at 2-3 bar, venting through the keyhole. After 30 minutes, the reactants were injected into the autoclave through the keyhole against a positive flow of CO_2. The key was then inserted into the autoclave, sealing it off from the atmosphere. At this point CO_2 was added, pressuring the system to 50 bar. Heat was then applied through the heating jacket, bringing the temperature to 65 °C. CO_2 was then added until the system pressure reached 275 bar. The moment the reaction temperature was reached was chosen as the starting point of the reaction.

2.6. Free-radical dispersion polymerisation of Styrene

The reaction was conducted with styrene (9.09 g, 10 ml), PDMS-MA stabiliser (20 wt% relative to styrene, 1.818 g) and AIBN initiator (2 wt% relative to styrene, 181.8 mg) in a 60 ml high pressure autoclave. Styrene and PDMS-MA with AIBN were degassed by bubbling with argon in separate vials for 30 minutes. During this time, the autoclave was

flushed with CO_2 at 2-3 bar, venting through the keyhole. After 30 minutes, styrene (10 ml, 9.09 g) was added to the PDMS-MA and AIBN and this mixture was injected into the autoclave through the keyhole against a positive flow of CO_2. The key was then inserted into the autoclave, sealing it off from the atmosphere. At this point CO_2 was added, pressuring the system to 50 bar. Heat was then applied through the heating jacket, bringing the temperature to 65 °C. CO_2 was then added until the system pressure reached 245 bar. The moment the reaction temperature was reached was chosen as the starting point of the reaction.

2.7. Free-radical precipitation polymerisation of PAA

The reaction was conducted with acrylic acid (2 g) and AIBN initiator (1.5 wt% relative to acrylic acid, 30 mg) in a 60 ml high pressure autoclave. Acrylic acid with AIBN was degassed by bubbling with argon in a glass vial for 30 minutes. During this time, the autoclave was flushed with CO_2 at 2-3 bar, venting through the keyhole. After 30 minutes, the acrylic acid and AIBN mixture was injected into the autoclave through the keyhole against a positive flow of CO_2. The key was then inserted into the autoclave, sealing it off from the atmosphere. At this point CO_2 was added, pressuring the system to 50 bar. Heat was then applied through the heating jacket, bringing the temperature to 62 °C. CO_2 was then added until the system pressure reached 160 bar. The moment the reaction temperature was reached was chosen as the starting point of the reaction.

2.8. Enzymatic ring-opening polymerisation of caprolactone

The reaction was conducted with CL (4 g, 35 mmol), HEMA (0.18 g, 1.40 mol) and Novozym-435 (0.4 g, 10 wt% relative to the caprolactone) in a 60 ml high pressure autoclave. HEMA and CL were loaded into the autoclave base, while Novozym beads were placed into a wire mesh cage affixed to the stirrer shaft described in previously[54]. The autoclave was degassed using a flow of CO_2 (3 bar, 15 min) through the keyhole, before being sealed and pressured to 50 bar. Heat was then applied through the heating jacket up to 65 °C. CO_2 was then added until the system pressure reached 207 bar. The moment the reaction temperature was reached was chosen as the starting point of the reaction.

3. Results and discussion

3.1. Dispersion polymerisation in $scCO_2$ of the model monomer MMA

3.1.1. Batch free-radical dispersion polymerisation of MMA

The batch approach was used to establish a reliable reaction progression curve, requiring a large amount of individual experiments. successive polymerisations were conducted with 1 wt% AIBN relative to MMA and were quenched by

crash cooling at 30-minute reaction time intervals, up to 240 minutes, based on the approximate total reaction time[27]. Analytical results of all reactions are available in the supporting information (SI-Table 1). The conversion as a function of reaction time shows the trend expected from literature, both in terms of reaction duration and a clear sigmoidal progression (*Fig. 3*). The sigmoidal progression is typical of a dispersion polymerisation with significant polymerisation occurring in the dispersed particle phase of the system[55].

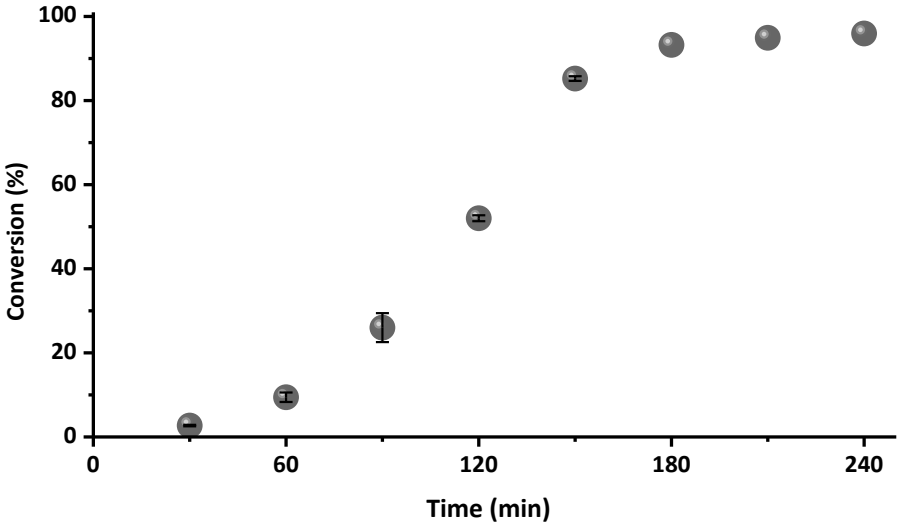

Fig. 3 *Conversion of MMA as a function of reaction time from sequential batch reactions quenched by crash cooling. Error bars represent the standard deviation of experimental conversion from 3 separate reactions. Reaction conditions: 10 ml of MMA, 0.468 g of PDMS-MA, 93.6 mg of AIBN, 220 bar and 65 ℃*

The molecular weight progression as a function of conversion showed a constant rise (*Fig. 4*), as has been observed previously[26-28]. The constant increase in average molar mass is due to the shift of the main polymerisation locus towards the growing dispersed phase, where longer chains are formed.

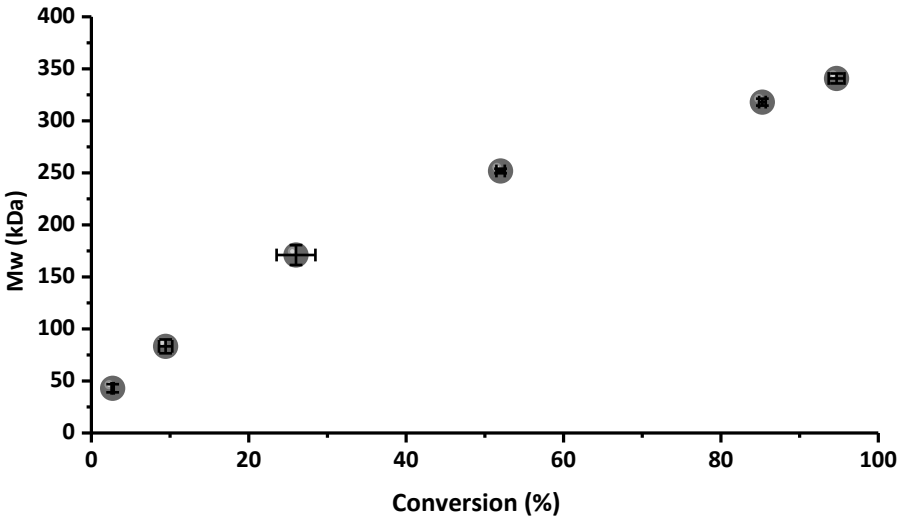

Fig. 4 *Mass-average molar mass in function of conversion from sequential batch reactions quenched by crash cooling. Error bars represent the standard deviation on data from 3 separate reactions. Reaction conditions: 10 ml of MMA, 0.468 g of PDMS-MA, 93.6 mg of AIBN, 220 bar and 65 ℃*

The final product, after 4 hours of reaction time, was a free-flowing white powder, consisting of discrete spherical particles with a diameter of 2566 ± 471 nm (SI-fig. 1). In summary, this is a very time and material demanding approach requiring eighteen separate reactions to acquire robust kinetic and product information. Our aim below is to show that this could be done better.

3.1.2. On-line monitoring of the free-radical dispersion polymerisation of MMA

While many on-line monitoring options are expensive and require specific setups, a readily available direct sampling approach from a single needle valve exit has been trialled before (Thurecht *et al.*[46]). Despite this method working for specific reactions, the uncontrolled nature of sample acquisition did cause significant issues. For the free-radical dispersion polymerisation of MMA, the volatile monomer was found to dissipate along with the CO_2 during the rapid release of pressure in the sample, resulting in erroneous conversion readings (SI Table 2, SI-fig. 2). From the GPC data it was however confirmed that the polymer in the sample was representative, by comparing to the previous quench data (SI-fig. 3). To avoid the loss of volatile compounds, we reasoned that a controlled sample depressurising method was required.

To keep costs low, the choice was made to avoid moving parts that could be used to slowly expand a sample volume, such as syringe pumps or manual pressure generators. The cylinder system (*Fig. 2*) was constructed to ensure no volatile compounds could be lost during sample expansion, but still allow for the immediate pressure release of the sample when desired. A fixed sample volume is obtained; the sample size being determined by the length of tubing used. As pressure is known to affect polymerisations in CO_2, it is important to know what pressure fluctuations are induced when extracting a sample. The pressure fluctuations of consecutive samples where measured at various pressures (SI-fig. 4)and we found that addition of 10-15 bar of CO_2 is needed prior to sampling. To aid in sample capture and recovery, a solvent is added to the cylinder prior to sampling. For MMA polymerisations $CDCl_3$ was used as the capturing solvent, as the deuterated solvent can then be used for immediate NMR analysis.

Reaction conditions were kept identical to the previously performed batch reactions, allowing a direct comparison of the obtained data. Utilising the cylinder system, samples were obtained at 30-minute intervals and this experiment was repeated 3 times to ensure reproducibility (*Fig. 5*). Sampling at 30 minutes of reaction time was not attempted, to

avoid disturbing the nucleation process of the polymerisation. Analytical results are tabulated in the supporting info (SI-Table 3).

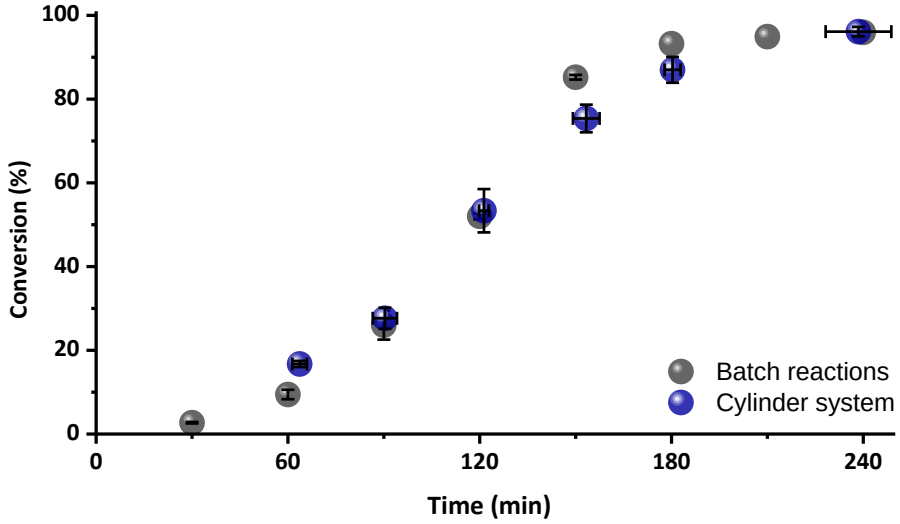

Fig. 5 *Conversion of MMA as a function of reaction time from samples obtained using the cylinder system compared to sequential batch reactions quenched by crash cooling. Error bars represent the standard deviation of experimental conversion from 3 separate reactions. Reaction conditions: 10 ml of MMA, 0.468 g of PDMS-MA, 93.6 mg of AIBN, 220 bar and 65 ℃*

A small apparent conversion discrepancy was observed after 150-180 minutes, but this is believed to be due to the partial drying of the polymer powder in the batch experiments. After 150 minutes of reaction time, the recovered product from the batch experiments was a free-flowing powder that was collected onto filter paper and transferred into a vial before conversion analysis via ^{1}H NMR. During this time, it is possible that residual monomer was lost, resulting in an artificially inflated conversion value. From comparison of the average molar mass, it can be further seen that the samples obtained using the cylinder system are representative of the ongoing polymerisation (*Fig. 6*). It is worth mentioning that the small volume of reactants removed, which is less than 30 mg per sample, is not expected to have a measurable effect on the reaction progression.

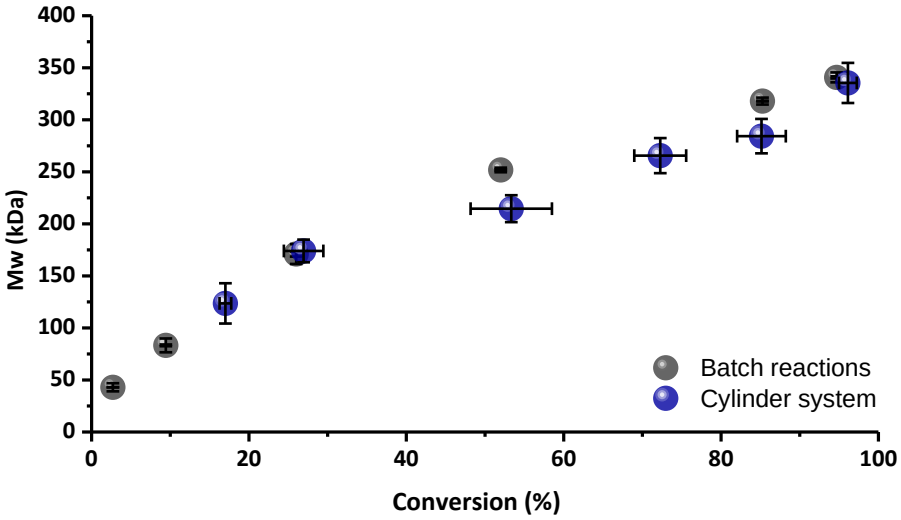

Fig. 6 *Mass average molar mass in function of conversion from samples obtained using the cylinder system compared to sequential batch reactions quenched by crash cooling. Error bars represent the standard deviation on data from 3 separate reactions. Reaction conditions: 10 ml of MMA, 0.468 g of PDMS-MA, 93.6 mg of AIBN, 220 bar and 65 ℃*

3.1.2.1. Kinetic modelling of the free-radical dispersion polymerisation of MMA

For facile and predictive modelling of the observed conversion trend, the cylinder system data was fitted to a model developed initially by Barrett and Thomas[55] and still used widely in modelling of sigmoidal conversion trends[31, 56-58]. This model assumes all polymerisation occurs in the dispersed polymer particle phase, which is the overwhelmingly dominant phase of the reaction under investigation[26]. Applying the steady-state hypothesis and assuming the volume of the dispersed phase is directly determined by the amount of polymer formed, this model generates the following equation pair:

$$\frac{d}{dt}x = \mathrm{k} \cdot \sqrt{x} \cdot (1 - x) \tag{1}$$

$$k = \alpha \cdot \sqrt{[M]_0 \cdot [I] \cdot V_p \cdot k_i} \cdot \frac{k_p}{\sqrt{k_t}} \tag{2}$$

By separating the initial component concentrations, a reduced rate constant k' was defined:

$$k' = \frac{k}{\sqrt{[M]_0 \cdot [I]}} = \alpha \cdot \sqrt{V_p \cdot k_i} \cdot \frac{k_p}{\sqrt{k_t}} \tag{3}$$

With the incorporation of an apparent induction time (t_0), integration of equation (1) leads to the following expression for conversion as a function of time:

$$x(t) = \begin{cases} 0\,, & t \le t_0 \\ \left(\frac{e^{kt} - e^{kt_0}}{e^{kt} + e^{kt_0}}\right)^2, & t > t_0 \end{cases} \tag{4}$$

The sigmoidal conversion curve from equation (4) was fitted to the experimental data obtained from the cylinder system (*Fig. 7*), with fitting variables set to $t_0 = 1800\ s$ and the lumped parameter $k' = 2.85 \cdot 10^{-3}\ M^{-1}s^{-1}$.

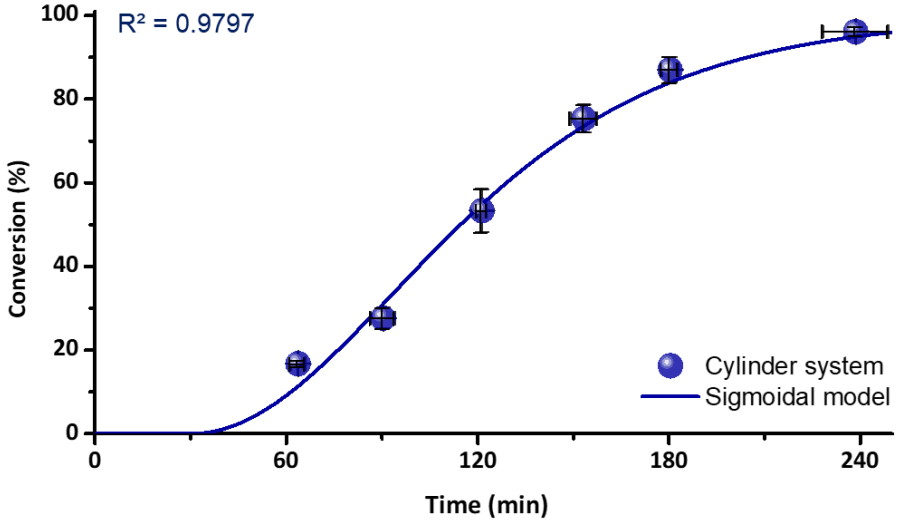

Fig. 7 *Sigmoidal model of conversion of MMA as a function of reaction time, fitted to conversion data obtained using the cylinder system. Error bars represent the standard deviation of experimental conversion from 3 separate reactions. Reaction conditions: 10 ml of MMA, 0.468 g of PDMS-MA, 93.6 mg of AIBN, 220 bar and 65 ℃. Model fitting variables:* $\boldsymbol{t_0 = 1800\ s}$, $\boldsymbol{k' = 2.85 \cdot 10^{-3}\ M^{-1}s^{-1}}$

The determined reduced rate constant k' is independent of initial component concentrations, allowing it to be used to predict the effect of changing initiator concentration on polymerisation progression. By maintaining the same fitting values and simply changing the initiator concentration value [I] in equation (2), a range of conversion curves were obtained for AIBN concentrations between 0.25 wt% and 2 wt% relative to MMA (SI-fig. 5). While detailed verification of the model quality using the batch quench method would require 21 separate reactions (using 200 g of MMA, 10 g of PDMS-MA and 1.8 g of AIBN), our use of the new cylinder system allowed model verification in just 3 reactions (using just 28 g of MMA, 1.4 g of PDMS-MA and 260 mg of AIBN) and also with a significant time saving! It was shown that the model was accurate across the tested AIBN concentration range, while the cylinder system was readily capable of on-line sampling under a range of varying conditions (SI-Table 4)(*Fig. 8*).

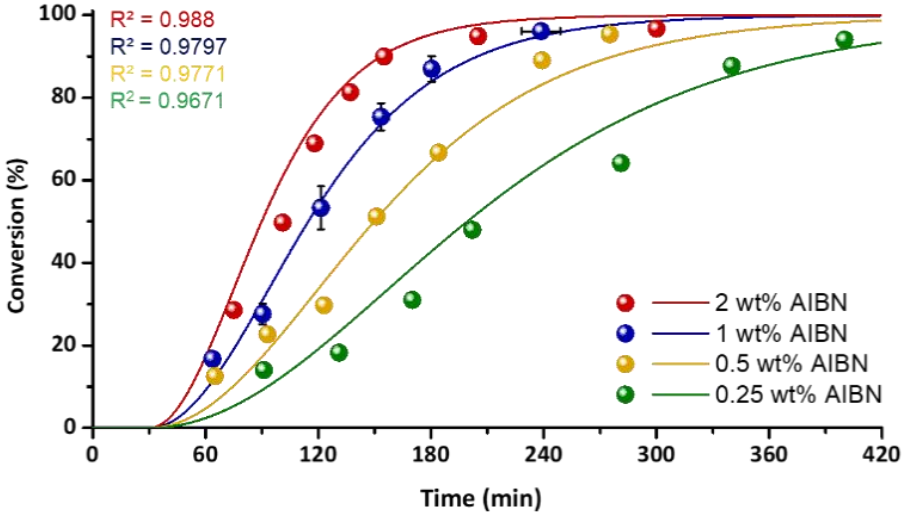

Fig. 8. *Conversion of MMA as a function of reaction time from samples obtained using the cylinder system (spheres) overlaying sigmoidal model predictions (lines) for various AIBN concentrations. Reaction conditions: 10 ml of MMA, 0.468 g of PDMS-MA, 23.4-187.2 mg of AIBN, 220 bar and 65 ℃. Model fitting variables:* $\boldsymbol{t_0 = 1800\ s}$, $\boldsymbol{k' = 2.85 \cdot 10^{-3}\ M^{-1}s^{-1}}$

3.1.3. On-line monitoring of the RAFT controlled dispersion polymerisation of MMA

Previous research has presented a kinetic study of RAFT control for the dispersion polymerisation of MMA in $scCO_2$, showing the efficacy of four different dithiobenzoate CTAs[24]. All four CTAs presented pseudo first-order kinetics, giving experimental molar masses close to the theoretical molar mass with a narrow dispersity of Đ≤1.30. these data mirrored well the control seen in solution polymerisations[24]. Successive batch reactions were quenched by crash cooling the reactor at set times, where samples at low conversion were collected by dissolving them in THF and then precipitating in cooled hexane. This methodology is rather laborious, time consuming and introduces considerable error, as each data point represents a different reaction. In addition, the monitoring at low conversion is compromised by the precipitation step, where short polymer chains can be lost. Thus we trialled the new cylinder sampling system was used as a more convenient and reliable monitoring system, for the RAFT controlled dispersion polymerisation of MMA using CPDT as the CTA.

The RAFT controlled polymerisation was successfully monitored using the cylinder system, with analytical data confirming that CPDT provided good control over the reaction (SI-Table 5). The final molar mass was found to be virtually equal to the theoretical prediction and a narrow polydispersity of Đ = 1.20 was achieved. GPC analysis of samples collected throughout the reaction show the controlled growth of the polymer chain with time, as seen by the unimodal peak shift to the left (*Fig. 9*).

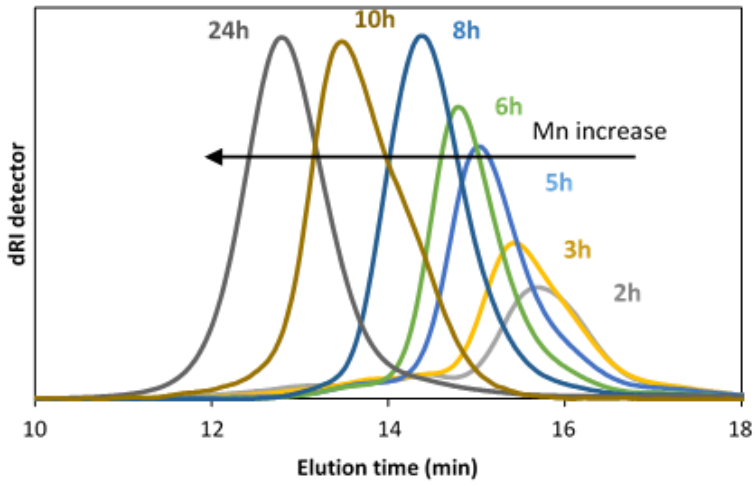

Fig. 9. *GPC traces showing the growth of PMMA in function of time in $scCO_2$ using CPDT as chain transfer agent. Reaction conditions:10 g of MMA, 0.5 g of PDMS-MA, 0.085 mmol of AIBN, 0.17 mmol of CPDT, 275 bar and 65 ℃*

The linear evolution of M_n as a function of conversion shows good agreement with pseudo-living behaviour, as the linear trend of the experimental data is closely aligned with the theoretical molecular weight increase. Livingness was further confirmed by the low polydispersity observed throughout the reaction, remaining below Đ ≤ 1.30 throughout (*Fig. 10*).

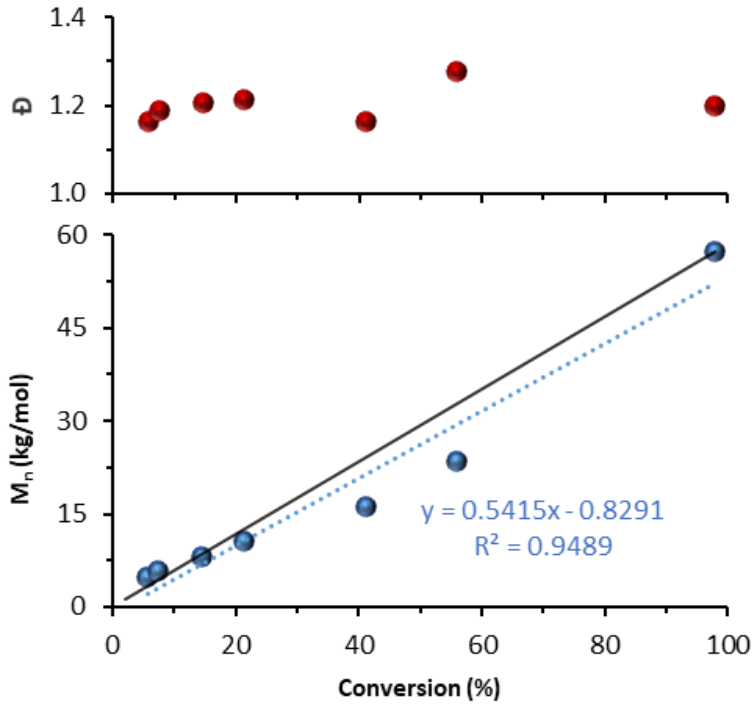

Fig. 10 *Evolution of M_n (blue) and Đ (red) as a function of conversion; solid trend line (black) is the theoretical M_n and dashed trend line (blue) is the linear fitting of experimental data. Reaction conditions: 10 g of MMA, 0.5 g of PDMS-MA, 0.085 mmol of AIBN, 0.17 mmol of CPDT, 275 bar and 65 ℃*

The logarithmic monomer conversion as a function of time provides important mechanistic insight, with two distinct regimes being observed for this reaction. The initial regime indicates mild retardation (*Fig. 11*). Retardation during RAFT polymerisation of methacrylates are commonly observed, although it tends to be more pronounced for polymerisation of acrylates or acrylamides[59]. From the experimental data an initial induction period of approximately 14 minutes was found. Gregory *et al.* previously reported induction periods of up to 12 hours for MMA polymerisation in $scCO_2$ with dithioester CTAs and no retardation[24]. It is important to reiterate that these data were obtained from quenched successive batch reactions where precipitation of the product in cold hexane might have excluded low molecular weight chains and artificially delayed the observation of the polymerisation onset. Therefore, the induction period was likely shorter. Long retardations are expected with other CTAs for example with the high stability of a dithioester intermediate radical. However, a shorter induction time should be expected for trithiocarbonate CTAs such as CPDT, owing to the less stable intermediate radicals[60]. This hypothesis aligns well with our experimental results.

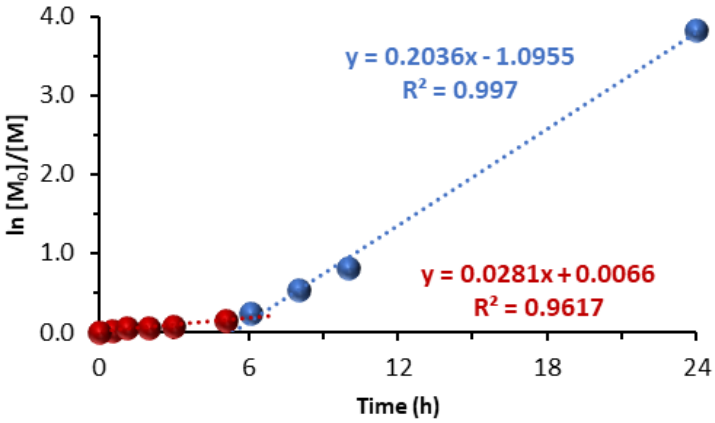

Fig. 11. *Pseudo-first-order kinetic plot of monomer conversion in function of reaction time for the dispersion polymerisation of MMA with CPDT in $scCO_2$. Two distinct reaction regimes are seen (red, blue). A 7.25-fold rate increase is seen between regimes.*

The second regime starts after 6 hours of reaction and presents a 7.25-fold increase in the rate of polymerisation compared to the previous regime. This could indicate the transition of the main reaction locus from the continuous phase into the dispersed phase. During the initial phase of a dispersion polymerisation, all reactants (*i.e.* monomer, initiator, etc.) are soluble in the continuous phase. Once the critical chain length (J_{crit}) is achieved, the polymer becomes insoluble and forms particles surrounded by the stabiliser, giving rise to a polymer-rich phase. As the particles grow, CO_2 and monomer can swell the particles, and the high concentration of monomer thus could cause the observed increase in polymerisation rate (Fig. 11). The pseudo-first-order kinetic plot remained linear throughout the second regime, up to 97.80% conversion, indicating once more successful RAFT control.

Using the cylinder system, the control of CPDT over the dispersion polymerisations of MMA was confirmed by conducting a single polymerisation. The experiment has also given some insights into the mechanism of the reaction, uncovering two distinct reaction regimes, possibly associated with the onset of nucleation. The facile application of the cylinder system led us quickly to findings that have provided a much better understanding of the polymerisations and to further develop in the area of controlled polymerisations in $scCO_2$ in an efficient and reproducible manner.

3.2. Monitoring of other reaction systems

To initiate the broader application of the cylinder system for reaction monitoring in supercritical fluids, the system suitability was tested for a selection of very different polymerisation reactions using the same setup.

3.2.1. Free-radical dispersion polymerisation of styrene

The use of a different monomer for the FRP dispersion polymerisation was first tested. Styrene has a much lower reactivity and very different monomer/polymer solubility in $scCO_2$[61, 62]. The styrene system was monitored successfully using the cylinder setup. $CDCl_3$ was used as the sample solvent, as it is a satisfactory solvent for styrene and polystyrene. While the polymerisation took more than 30 hours to reach above 95% conversion, the cylinder system allowed for on-line tracking of the reaction progress. Initial samples confirmed the lower reactivity of this system, while later samples allowed for real-time determination of the point at which the desired conversion was reached (*Fig. 12*). Using equation (4), an initial fitting of the data was also achieved, showing the expected sigmoidal progression of conversion.

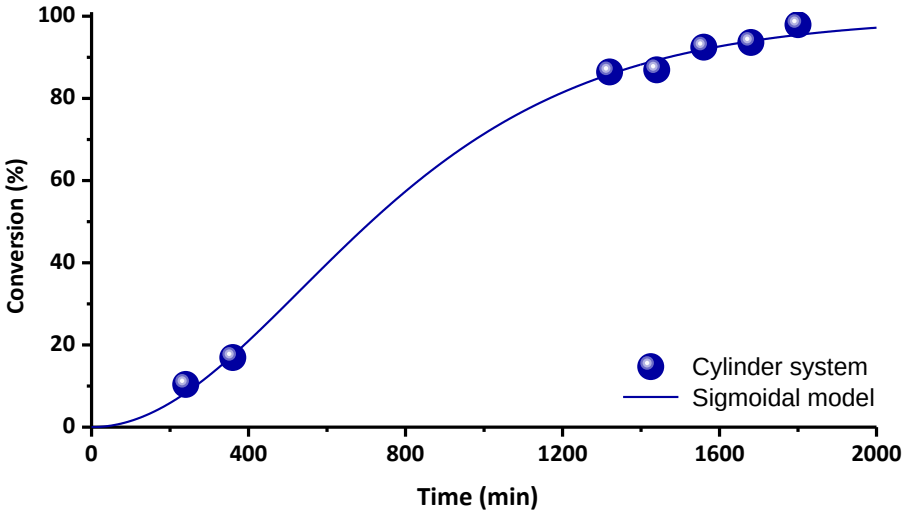

Fig. 12 *Conversion of Styrene as a function of reaction time from samples obtained using the cylinder system overlaying a sigmoidal model fitting line. Reaction conditions: 10 ml of Styrene, 1.818 g of PDMS-MA, 181.8 mg of AIBN, 245 bar and 65 ℃. Model fitting variables:* $\boldsymbol{t_0 = 0\ s,\ k' = 2.40 \cdot 10^{-4}\ M^{-1}s^{-1}}$

3.2.2. Free-radical precipitation polymerisation of acrylic acid

The precipitation polymerisation of acrylic acid is a reaction that does not use a stabiliser to guarantee a consistent reaction mixture. The reaction has also been kinetically analysed previously by Ollagnier *et al.*[31] using in-situ IR as monitoring technique, allowing for a clear comparison of observed conversion. Acrylic acid is soluble in water, so D_2O was chosen as the solvent to add into the cylinder system. The high molar mass poly(acrylic acid) formed in this reaction is generally poorly soluble, meaning that NMR analysis would be delayed until solution was achieved. To remedy this issue, methanol was added to the D_2O as an internal standard.

A stock solution of D_2O and methanol was used throughout the experiment and an initial sample was taken to establish the ratio between acrylic acid and methanol in a fully unpolymerized sample. The relative reduction in acrylic acid with respect to methanol in subsequent samples was then used to determine conversion. The observed conversion trend was then compared to the fitted kinetic model from Ollagnier and co-workers[31], showing that the cylinder system provides the same accurate data(*Fig. 13*).

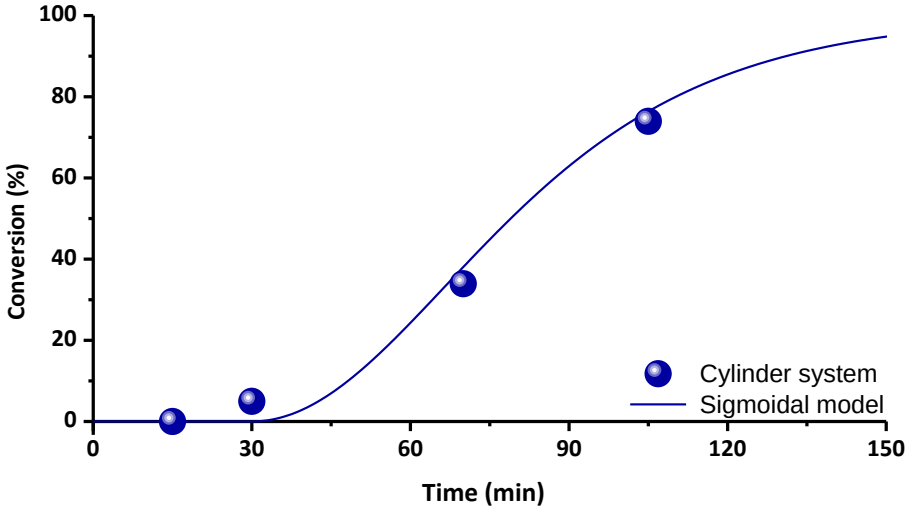

Fig. 13 *Conversion of Acrylic acid as a function of reaction time from samples obtained using the cylinder system overlaying a sigmoidal model fitting line with fitting variables from Ollagnier et al.[31]. Reaction conditions: 2 g of acrylic acid, 30 mg of AIBN, 160 bar and 62 ℃. Model fitting variables:* $\boldsymbol{t_0 = 1800\ s}$, $\boldsymbol{k' = 1.60 \cdot 10^{-2}\ M^{-1}s^{-1}}$

3.2.3. Enzymatic ring-opening polymerisation of caprolactone

In an attempt to investigate the kinetics of two simultaneous competing reactions, the HEMA initiated eROP of ε-caprolactone in $scCO_2$ was studied. The hydroxyl group of HEMA can act as an initiator in ROP to yield functional polymers[63, 64]. While in the presence of Novozym 435, HEMA is known to undergo transesterification with itself, resulting in a lack of control over the polymers produced[65, 66]. Utilising the cylinder system, both transesterification

and polymerisation were monitored simultaneously, showcasing that competing reactions can be monitored simultaneously in-situ. $CDCl_3$ was used as the sample solvent since it is suitable for HEMA, CL, and pCL. Analysis of the reaction mixture samples showed the expected increase in both polymerisation and transesterification in function of time (*Fig. 14*).

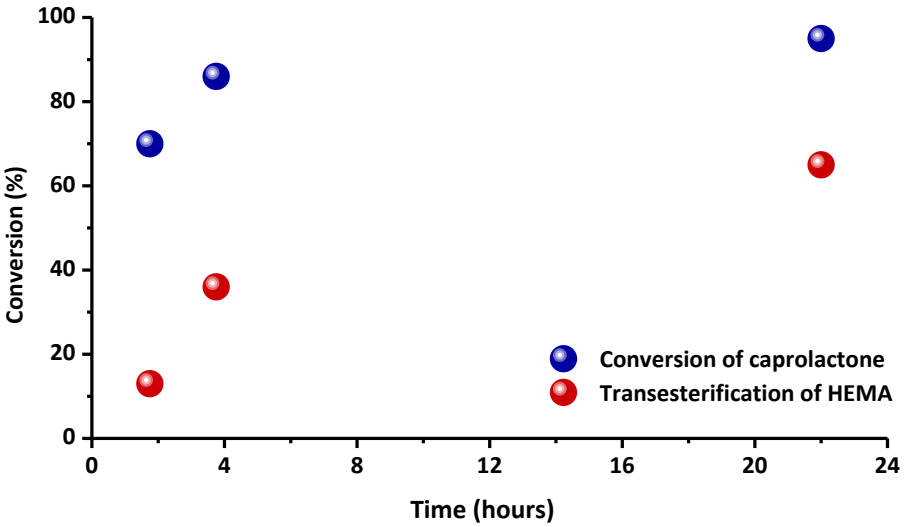

Fig. 14 *Conversion in function of reaction time for the polymerisation of caprolactone and the concurrent transesterification of HEMA. Reaction conditions: 4 g of CL, 0.18 g of HEMA, 0.4 g of Novozym 435, 207 bar and 65 ℃.*

While further investigation of this reaction system is beyond the scope of this research, it is clear that the new cylinder sampling system is capable of monitoring a more complex reaction mixture with two competing reactions in an expanded bulk.

4. Conclusions

Accessible on-line reaction monitoring is crucial for reproducible and efficient research of chemical reactions and especially polymerisations. In this paper we have developed an inexpensive and reliable on-line monitoring system for reactions in $scCO_2$, using only readily commercially available parts. The efficacy was first confirmed for the widely studied dispersion polymerisation of MMA, by comparing conversion and molar mass trends to known values. After kinetic modelling, the rapid data gathering capabilities were highlighted by varying initiator concentration for the dispersion polymerisation of MMA. The wide applicability of the cylinder system was then tested by monitoring a range of very different polymerisations and reactions at various conditions. The ability to easily add an internal standard for the monitoring of acrylic acid conversion, highlighted the facile and adaptable applicability of the developed cylinder system.

5. Acknowledgements

AACP is co-funded through a SINCHEM Grant. SINCHEM is a Joint Doctorate programme selected under the Erasmus Mundus Action 1 Programme (FPA 2013-0037). We would like to thank Mark Guyler and Richard Wilson for all their technical assistance and advice in constructing the cylinder system.

6. References

[1] H. Minato, M. Iwakawa, Generation of Free Radicals at Subzero Temperatures. IV.1 On the Mechanism of Generation of Free Radicals from the Sodium Formaldehyde Sulfoxylate—Iron—Hydroperoxide System, Polymer Journal, 6 (1974) 234, 10.1295/polymj.6.234.
[2] P. Nesvadba, Radical Polymerization in Industry, in: Encyclopedia of Radicals in Chemistry, Biology and Materials, John Wiley & Sons, Ltd., 2012, pp. 1-36, 10.1002/9781119953678.rad080.
[3] J. Kendall, D. Canelas, J. Young, J. Desimone, Polymerizations in supercritical carbon dioxide, in: Chem. Rev., 1999, pp. 543-563, 10.1021/cr9700336.
[4] A. Millner, H. Ollivier, Beliefs, Politics, and Environmental Policy, Review of Environmental Economics and Policy, 10 (2016) 226-244, 10.1093/reep/rew010.
[5] S. Krishna Mohan, Green solvents for polymerization of methyl methacrylate to poly(methyl methacrylate), in: Green Solvents I: Properties and Applications in Chemistry, 2012, pp. 251-298, 10.1007/978-94-007-1712-1_9.
[6] T.D. McAllister, L.D. Farrand, S.M. Howdle, Improved Particle Size Control for the Dispersion Polymerization of Methyl methacrylate in Supercritical Carbon Dioxide, Macromolecular Chemistry and Physics, 217 (2016) 2294-2301, 10.1002/macp.201600131.
[7] B. Metz, O. Davidson, H. de Coninck, M. Loos, L. Meyer, IPCC Special Report on Carbon Dioxide Capture and Storage, in: Annex 1: Properties of CO_2 and carbon-based fuels, IPCC, Cambridge, UK, 2005, pp. 387-388,
[8] A.I. Cooper, Polymer synthesis and processing using supercritical carbon dioxide, Journal of Materials Chemistry, 10 (2000) 207-234, 10.1039/a906486i.
[9] F. Rindfleisch, T.P. DiNoia, M.A. McHugh, Solubility of Polymers and Copolymers in Supercritical CO2, The Journal of Physical Chemistry, 100 (1996) 15581-15587, 10.1021/jp9615823.
[10] C. Domingo, A. Vega, M.A. Fanovich, C. Elvira, P. Subra, Behavior of poly(methyl methacrylate)–based systems in supercritical CO2 and CO2 plus cosolvent: Solubility measurements and process assessment, Journal of Applied Polymer Science, 90 (2003) 3652-3659, doi:10.1002/app.13097.
[11] J.M. DeSimone, E.E. Maury, Y.Z. Menceloglu, J.B. McClain, T.J. Romack, J.R. Combes, Dispersion Polymerizations in Supercritical Carbon Dioxide, Science, 265 (1994) 356-359, 10.1126/science.265.5170.356.
[12] J.M. DeSimone, J.S. Keiper, Surfactants and self-assembly in carbon dioxide, Current Opinion in Solid State and Materials Science, 5 (2001) 333-341, https://doi.org/10.1016/S1359-0286(00)00041-3.
[13] P. Christian, M.R. Giles, R.M.T. Griffiths, D.J. Irvine, R.C. Major, S.M. Howdle, Free radical polymerization of methyl methacrylate in supercritical carbon dioxide using a pseudo-graft stabilizer: effect of monomer, initiator, and stabilizer concentrations, Macromolecules, 33 (2000) 9222-9227, 10.1021/ma0008948.
[14] P. Christian, M.R. Giles, R.M.T. Griffiths, D.J. Irvine, R.C. Major, S.M. Howdle, Free Radical Polymerization of Methyl Methacrylate in Supercritical Carbon Dioxide Using a Pseudo-Graft Stabilizer: Effect of Monomer, Initiator, and Stabilizer Concentrations, Macromolecules, 33 (2000) 9222-9227, 10.1021/ma0008948.
[15] M.R. Giles, S.M. Howdle, New unsaturated surfactants for the dispersion polymerisation of methyl methacrylate in supercritical carbon dioxide, European Polymer Journal, 37 (2001) 1347-1351, https://doi.org/10.1016/S0014-3057(00)00258-5.
[16] P.F. Oliveira, R.A.F. Machado, D. Barth, E.D. Acosta, Dispersion polymerization of methyl methacrylate in supercritical carbon dioxide using vinyl terminated poly(dimethylsiloxane), Chemical Engineering and Processing: Process Intensification, 103 (2016) 46-52, https://doi.org/10.1016/j.cep.2015.10.022.
[17] S.H. Han, K.K. Park, S.H. Lee, Polymerization of methyl methacrylate in carbon dioxide using glycidyl methacrylate linked reactive stabilizer: Effect of pressure, reaction time, and mixing, Macromolecular Research, 17 (2009) 51-57, 10.1007/BF03218601.
[18] P.B. Zetterlund, F. Aldabbagh, M. Okubo, Controlled/living heterogeneous radical polymerization in supercritical carbon dioxide, Journal of Polymer Science Part A: Polymer Chemistry, 47 (2009) 3711-3728, 10.1002/pola.23432.

[19] R. McHale, F. Aldabbagh, P.B. Zetterlund, M. Okubo, Nitroxide-Mediated Radical Dispersion Polymerization of Styrene in Supercritical Carbon Dioxide Using a Poly(dimethylsiloxane-block-styrene) Alkoxyamine as Initiator and Stabilizer, Macromolecular Rapid Communications, 27 (2006) 1465-1471, 10.1002/marc.200600383.
[20] J. Ryan, F. Aldabbagh, P.B. Zetterlund, M. Okubo, First nitroxide-mediated free radical dispersion polymerizations of styrene in supercritical carbon dioxide, Polymer, 46 (2005) 9769-9777, https://doi.org/10.1016/j.polymer.2005.08.039.
[21] B. Grignard, C. Jérôme, C. Calberg, R. Jérôme, C. Detrembleur, Atom transfer radical polymerization of MMA with a macromolecular ligand in a fluorinated solvent and in supercritical carbon dioxide, European Polymer Journal, 44 (2008) 861-871, https://doi.org/10.1016/j.eurpolymj.2007.11.020.
[22] S. Villarroya, K.J. Thurecht, A. Heise, S.M. Howdle, Supercritical CO2: an effective medium for the chemo-enzymatic synthesis of block copolymers?, Chemical Communications, (2007) 3805-3813, 10.1039/B701128H.
[23] T. Arita, S. Beuermann, M. Buback, P. Vana, RAFT Polymerization of Methyl Acrylate in Carbon Dioxide, Macromolecular Materials and Engineering, 290 (2005) 283-293, 10.1002/mame.200400274.
[24] A.M. Gregory, K.J. Thurecht, S.M. Howdle, Controlled Dispersion Polymerization of Methyl Methacrylate in Supercritical Carbon Dioxide via RAFT, Macromolecules, 41 (2008) 1215-1222, 10.1021/ma702017r.
[25] P.A. Mueller, G. Storti, M. Morbidelli, The reaction locus in supercritical carbon dioxide dispersion polymerization. The case of poly(methyl methacrylate), Chemical Engineering Science, 60 (2005) 377-397, 10.1016/j.ces.2004.07.122.
[26] C. Chatzidoukas, P. Pladis, C. Kiparissides, Mathematical modeling of dispersion polymerization of methyl methacrylate in supercritical carbon dioxide, Industrial and Engineering Chemistry Research, 42 (2003) 743-751, 10.1021/ie020397a.
[27] P.A. Mueller, G. Storti, M. Morbidelli, Detailed modelling of MMA dispersion polymerization in supercritical carbon dioxide, Chemical Engineering Science, 60 (2005) 1911, 10.1016/j.ces.2004.11.029.
[28] P.A. Mueller, G. Storti, M. Morbidelli, C.A. Mantelis, T. Meyer, Dispersion Polymerization of Methyl Methacrylate in Supercritical Carbon Dioxide: Control of Molecular Weight Distribution by Adjusting Particle Surface Area, Macromolecular Symposia, 259 (2007) 218-225, 10.1002/masy.200751326.
[29] P. López-Domínguez, J.E. Rivera-Peláez, G. Jaramillo-Soto, J.F. Barragán-Aroche, E. Vivaldo-Lima, Modeling of RAFT polymerization of MMA in supercritical carbon dioxide using the PC-SAFT equation of state, Reaction Chemistry & Engineering, 5 (2020) 547-560, 10.1039/C9RE00461K.
[30] J.J. Haven, T. Junkers, Online Monitoring of Polymerizations: Current Status, European Journal of Organic Chemistry, 2017 (2017) 6474-6482, 10.1002/ejoc.201700851.
[31] J. Ollagnier, T. Tassaing, S. Harrisson, M. Destarac, Application of online infrared spectroscopy to study the kinetics of precipitation polymerization of acrylic acid in supercritical carbon dioxide, React. Chem. Eng., 1 (2016) 372-378, 10.1039/c6re00022c.
[32] P. Lacroix-Desmazes, A. Guyot, Reactive surfactants in heterophase polymerization, Colloid and Polymer Science, 274 (1996) 1129-1136, 10.1007/BF00655683.
[33] S. Shen, E.D. Sudol, M.S. El-Aasser, Dispersion polymerization of methyl methacrylate: Mechanism of particle formation, Journal of Polymer Science Part A: Polymer Chemistry, 32 (1994) 1087-1100, 10.1002/pola.1994.080320611.
[34] M.H.G.M. Penders, A. Vrij, A turbidity study on colloidal silica particles in concentrated suspensions using the polydisperse adhesive hard sphere model, The Journal of Chemical Physics, 93 (1990) 3704-3711, 10.1063/1.458799.
[35] U. Fehrenbacher, M. Ballauff, Kinetics of the early stage of dispersion polymerization in supercritical CO 2 as monitored by turbidimetry. 2. Particle formation and locus of polymerization, Macromolecules, 35 (2002) 3653-3661, 10.1021/ma011985n.
[36] G. Li, M.Z. Yates, K.P. Johnston, S.M. Howdle, In-Situ Investigation on the Mechanism of Dispersion Polymerization in Supercritical Carbon Dioxide, Macromolecules, 33 (2000) 4008-4014, 10.1021/ma9921504.
[37] M.L. O'Neill, M.Z. Yates, K.P. Johnston, C.D. Smith, S.P. Wilkinson, Dispersion Polymerization in Supercritical CO2 with a Siloxane-Based Macromonomer: 1. The Particle Growth Regime, Macromolecules, 31 (1998) 2838-2847, 10.1021/ma971314i.
[38] M.L. O'Neill, M.Z. Yates, K.P. Johnston, C.D. Smith, S.P. Wilkinson, Dispersion Polymerization in Supercritical CO2 with Siloxane-Based Macromonomer. 2. The Particle Formation Regime, Macromolecules, 31 (1998) 2848-2856, 10.1021/ma971315a.
[39] J.R. Richards, J.P. Congalidis, Measurement and control of polymerization reactors, Computers & Chemical Engineering, 30 (2006) 1447-1463, https://doi.org/10.1016/j.compchemeng.2006.05.021.
[40] B. Grignard, B. Gilbert, C. Malherbe, C. Jérôme, C. Detrembleur, Online Monitoring of Heterogeneous Polymerizations in Supercritical Carbon Dioxide by Raman Spectroscopy, ChemPhysChem, 13 (2012) 2666-2670, 10.1002/cphc.201200373.

[41] S.M. Howdle, K. Stanley, V.K. Popov, V.N. Bagratashvili, Can High-Pressure Raman Spectroscopy Be Simplified? A Microscale Optical-Fiber Capillary Cell for the Study of Supercritical Fluids, Appl. Spectrosc., 48 (1994) 214-218, https://doi.org/10.1366/0003702944028434.
[42] W. Wang, R.M.T. Griffiths, M.R. Giles, P. Williams, S.M. Howdle, Monitoring dispersion polymerisations of methyl methacrylate in supercritical carbon dioxide, European Polymer Journal, 39 (2003) 423-428, 10.1016/S0014-3057(02)00249-5.
[43] C.A. Mantelis, T. Meyer, Supercritical reaction calorimetry: Versatile tool for measuring heat transfer properties and monitoring chemical reactions in supercritical fluids, Industrial and Engineering Chemistry Research, 47 (2008) 3372-3379, 10.1021/ie0712030.
[44] S. Jiang, E.D. Sudol, V.L. Dimonie, M.S. El-Aasser, Kinetics of dispersion polymerization: Effect of medium composition, Journal of Polymer Science Part A: Polymer Chemistry, 46 (2008) 3638-3647, 10.1002/pola.22704.
[45] S. Jiang, E.D. Sudol, V.L. Dimonie, M.S. El-Aasser, Kinetics of dispersion polymerization of methyl methacrylate and n-butyl acrylate: Effect of initiator concentration, Macromolecules, 40 (2007) 4910-4916, 10.1021/ma062679i.
[46] K.J. Thurecht, S. Villarroya, J. Zhou, S.M. Howdle, A. Heise, M. Degeus, M.F. Wyatt, Kinetics of enzymatic ring-opening polymerization of ε-caprolactone in supercritical carbon dioxide, Macromolecules, 39 (2006) 7967-7972, 10.1021/ma061310q.
[47] W.F. Reed, A.M. Alb, Monitoring Polymerization Reactions: From Fundamentals to Applications, 2014, 10.1002/9781118733813.
[48] S. Bilgin, R. Tomovska, J.M. Asua, Surfactant-free high solids content polymer dispersions, Polymer, 117 (2017) 64-75, https://doi.org/10.1016/j.polymer.2017.04.014.
[49] D.A. Paquet, W.H. Ray, Tubular reactors for emulsion polymerization: I. Experimental investigation, AIChE Journal, 40 (1994) 73-87, doi:10.1002/aic.690400110.
[50] M. Alauhdin, T.M. Bennett, G. He, S.P. Bassett, G. Portale, W. Bras, D. Hermida-Merino, S.M. Howdle, Monitoring morphology evolution within block copolymer microparticles during dispersion polymerisation in supercritical carbon dioxide: a high pressure SAXS study, Polymer Chemistry, 10 (2019) 860-871, 10.1039/c8py01578c.
[51] J. Jennings, M. Beija, A.P. Richez, S.D. Cooper, P.E. Mignot, K.J. Thurecht, K.S. Jack, S.M. Howdle, One-Pot Synthesis of Block Copolymers in Supercritical Carbon Dioxide: A Simple Versatile Route to Nanostructured Microparticles, Journal of the American Chemical Society, 134 (2012) 4772-4781, 10.1021/ja210577h.
[52] T.A. Hoefling, R.M. Enick, E.J. Beckman, Microemulsions in near-critical and supercritical carbon dioxide, The Journal of Physical Chemistry, 95 (1991) 7127-7129, 10.1021/j100172a006.
[53] T. Liu, J.M. Desimone, G.W. Roberts, Kinetics of the precipitation polymerization of acrylic acid in supercritical carbon dioxide: The locus of polymerization, Chemical Engineering Science, 61 (2006) 3129-3139, 10.1016/j.ces.2005.11.052.
[54] F.C. Loeker, C.J. Duxbury, R. Kumar, W. Gao, R.A. Gross, S.M. Howdle, Enzyme-Catalyzed Ring-Opening Polymerization of ε-Caprolactone in Supercritical Carbon Dioxide, Macromolecules, 37 (2004) 2450-2453, 10.1021/ma0349884.
[55] K.E.J. Barrett, H.R. Thomas, Kinetics of dispersion polymerization of soluble monomers. I. Methyl methacrylate, Journal of Polymer Science Part A-1: Polymer Chemistry, 7 (1969) 2621-2650, 10.1002/pol.1969.150070913.
[56] L.I. Costa, G. Storti, Kinetic Modeling of Precipitation and Dispersion Polymerizations, in: W. Pauer (Ed.) Polymer Reaction Engineering of Dispersed Systems: Volume II, Springer International Publishing, Cham, 2018, pp. 45-77, 10.1007/12_2017_13.
[57] K. Matyjaszewski, J. Spanswick, Atom Transfer Radical Polymerization (ATRP), in: Reference Module in Materials Science and Materials Engineering, Elsevier, 2016, https://doi.org/10.1016/B978-0-12-803581-8.01354-0.
[58] B. Akpinar, L.A. Fielding, V.J. Cunningham, Y. Ning, O.O. Mykhaylyk, P.W. Fowler, S.P. Armes, Determining the Effective Density and Stabilizer Layer Thickness of Sterically Stabilized Nanoparticles, Macromolecules, 49 (2016) 5160-5171, 10.1021/acs.macromol.6b00987.
[59] G. Moad, E. Rizzardo, S.H. Thang, Towards living radical polymerisation, Acc. Chem. Res., 41 (2008),
[60] G. Moad, E. Rizzardo, S.H. Thang, Living Radical Polymerization by RAFT Process, Aust. J. Chem, 58 (2005) 379-410,
[61] D.A. Canelas, D.E. Betts, J.M. DeSimone, Dispersion Polymerization of Styrene in Supercritical Carbon Dioxide: Importance of Effective Surfactants, Macromolecules, 29 (1996) 2818-2821, 10.1021/ma951642n.
[62] A.V. Ewing, S.G. Kazarian, Current trends and opportunities for the applications of in situ vibrational spectroscopy to investigate the supercritical fluid processing of polymers, The Journal of Supercritical Fluids, 134 (2018) 88-95, https://doi.org/10.1016/j.supflu.2017.12.011.
[63] P. Dubois, R. Jerome, P. Teyssie, Macromolecular engineering of polylactones and polylactides. 3. Synthesis, characterization, and applications of poly(iε-caprolactone) macromonomers, Macromolecules, 24 (1991) 977-981, 10.1021/ma00005a002.

[64] G. Englezou, K. Kortsen, A.A.C. Pacheco, R. Cavanagh, J.C. Lentz, E. Krumins, C. Sanders-Velez, S.M. Howdle, A.J. Nedoma, V. Taresco, 2-Methyltetrahydrofuran (2-MeTHF) as a versatile green solvent for the synthesis of amphiphilic copolymers via ROP, FRP, and RAFT tandem polymerizations, Journal of Polymer Science, n/a (2020), 10.1002/pol.20200183.
[65] M. Takwa, Y. Xiao, N. Simpson, E. Malmström, K. Hult, C.E. Koning, A. Heise, M. Martinelle, Lipase Catalyzed HEMA Initiated Ring-Opening Polymerization: In Situ Formation of Mixed Polyester Methacrylates by Transesterification, Biomacromolecules, 9 (2008) 704-710, 10.1021/bm7010449.
[66] Y. Xiao, M. Takwa, K. Hult, C.E. Koning, A. Heise, M. Martinelle, Systematic Comparison of HEA and HEMA as Initiators in Enzymatic Ring-Opening Polymerizations, Macromolecular Bioscience, 9 (2009) 713-720, 10.1002/mabi.200800290.

On-line polymerisation monitoring in $scCO_2$: a reliable and inexpensive sampling method in high pressure applications

Kristoffer Kortsen[a], Ana A.C. Pacheco[a], Joachim C Lentz[a], Vincenzo Taresco[a], Steven M. Howdle[a,*]

[a] University of Nottingham, School of Chemistry, University Park, NG7 2RD, UK

[*] Corresponding author. E-mail address: steve.howdle@Nottingham.ac.uk

Supporting information

Table 1 Results of batch polymerisation reactions quenched by crash cooling at 30-minute reaction time intervals. Reaction conditions: 10 ml of MMA, 0.468 g of PDMS-MA, 93.6 mg of AIBN, 220 bar and 65 ℃
a – determined via ^{1}H NMR, b – determined via GPC

Reaction time (min)	Conversion (%)[a]	M_n (kDa)[b]	M_w (kDa)[b]	Đ[b]	Product consistency
30	2.6	19.7	37	1.88	Liquid
30	2.6	18.7	48.5	2.59	Liquid
30	2.9	20.5	43.3	2.11	Liquid
60	10.7	32.9	89.3	2.72	Liquid
60	9.1	35.4	87	2.46	Liquid
60	8.5	28.3	73.2	2.59	Liquid
90	29.1	64.8	183.1	2.83	Viscous liquid
90	22.3	49.3	156.7	3.18	Viscous liquid
90	26.6	57.9	173.2	2.99	Viscous liquid
120	52.5	86.2	254.3	2.95	Cloudy gel
120	51.2	85	248.4	2.92	Cloudy gel
120	52.3	92.7	252.5	2.72	Cloudy gel
150	84.8	133	323.0	2.43	powder
150	85.1	119.9	317.7	2.65	Powder
150	85.9	124.5	313.2	2.52	Powder
180	93.2	167.4	345.6	2.06	Powder
210	94.9	157.9	333.5	2.11	Powder
240	96	168.4	342.9	2.04	Powder

Fig. 1 SEM image of PDMS-MA stabilised PMMA particles formed after 240 minutes of reaction time, showing distinct spherical morphology with an average particle diameter of 2566 ± 471 nm.

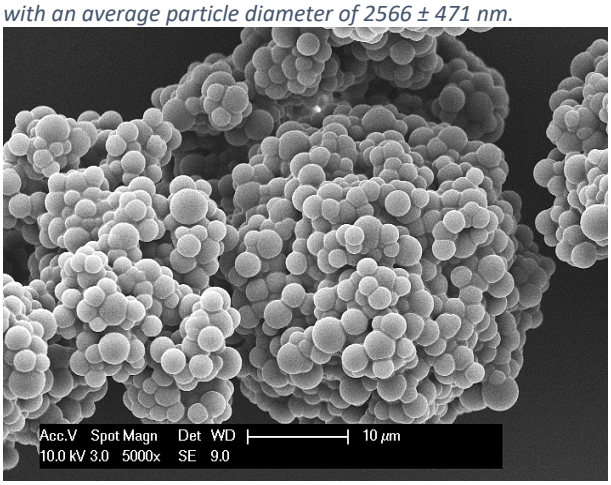

Table 2 Sample results of polymerisation reactions monitored using a singular needle valve sampling system. Reaction conditions: 10 ml of MMA, 0.468 g of PDMS-MA, 93.6 mg of AIBN, 220 bar and 65 ℃
a – determined via ^{1}H NMR, b – determined via GPC

Reaction time (min)	Conversion (%)[a]	M_n (kDa)[b]	M_w (kDa)[b]	Đ[b]
10	24.1	-	-	-
13	6.3	-	-	-
20	13.0	-	-	-
23	33.5	15.6	26.3	1.69
30	58.3	14.9	29.5	1.98
30	77.2	28.6	58.4	2.05
33	84.8	20.6	47.0	2.28
40	86.3	16.5	53.8	3.27
43	82.1	22.7	65.4	2.88
45	80.5	35.7	98.7	2.76
50	85.7	18.5	54.7	2.96
53	81.6	26.5	79.4	2.99
60	79.3	54.5	155.0	2.85
60	79.2	20.6	56.0	2.72
63	87.1	30.6	95.9	3.13
70	82.6	24.5	69.9	2.85
73	83.7	43.3	136.2	3.15
75	88.6	68.1	192.2	2.82
83	82.3	47.5	153.0	3.22
88	83.4	32.7	115.2	3.53
90	89.9	65.5	190.6	2.91
93	85.4	54.8	177.1	3.23
103	85.9	41.1	137.2	3.34
118	82.7	52.0	165.2	3.17
120	95.6	79.1	232.2	2.93
123	89.3	91.7	309.8	3.38
138	91.5	62.8	241.0	3.84
150	98.1	91.3	266.5	2.92
153	94.4	67.7	254.4	3.76
158	95.0	78.6	274.4	3.49
180	98.6	78.8	245.9	3.12
183	96.1	84.1	305.3	3.63
188	95.0	80.1	282.0	3.52
230	98.2	143.3	316.3	2.21
240	90.4	138.6	386.7	2.79
240	96.6	160.8	366.0	2.28

Fig. 2 Conversion as a function of time for on-line sampling using a singular needle valve sampling system (red), compared to results from the batch quench experiments (grey). The single valve sampling approach results in artificially high conversion measurements, due to the loss of volatile monomer upon retrieval of the sample.

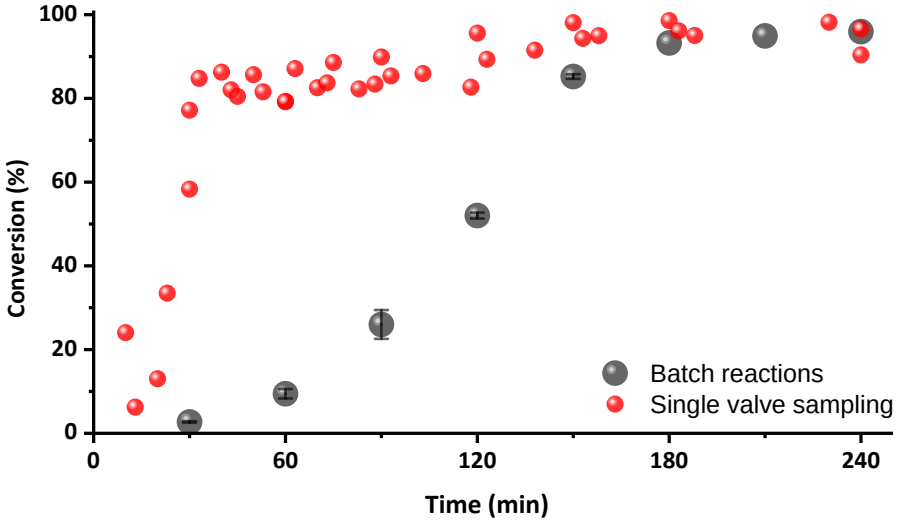

Fig. 3 Mass average molar mass as a function of reaction time for on-line sampling using a singular needle valve, compared to results from the quench experiments. The single valve sampling system provides representative molecular weight data, despite the loss of monomer in the method.

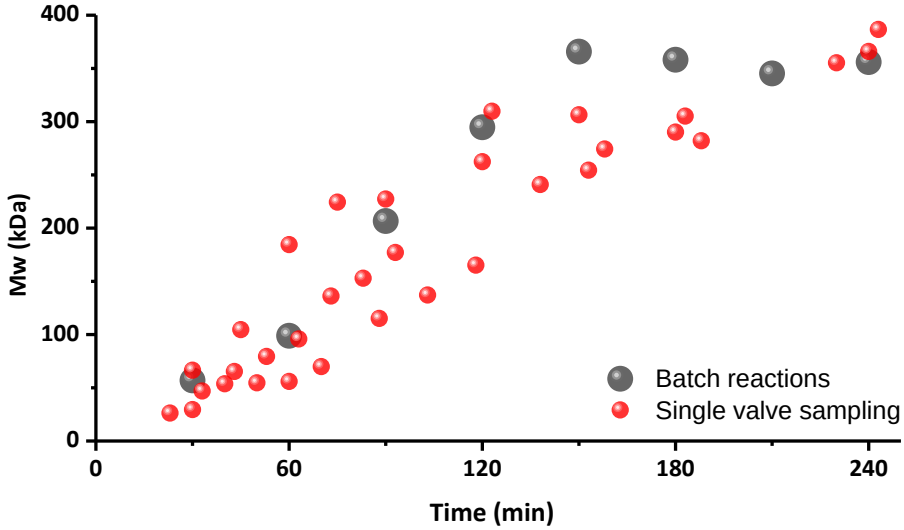

Fig. 4 Observed pressure progression during consecutive samplings, using the cylinder. Orange spheres denote the observed pressure drop immediately after sampling, blue spheres denote the pressure recovery as the system stabilises.

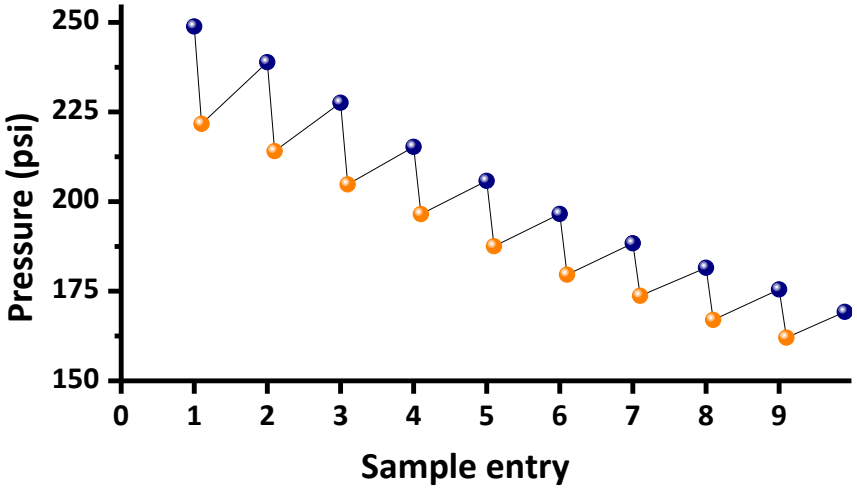

Table 3 Data obtained from samples of polymerisation reactions monitored using the cylinder system. Reaction conditions: 10 ml of MMA, 0.468 g of PDMS-MA, 93.6 mg of AIBN, 220 bar and 65 ℃
a – determined via ^{1}H NMR, b – determined via GPC

Reaction time (min)	Conversion (%)[a]	M_n (kDa)[b]	M_w (kDa)[b]	Đ[b]
61	16.2	36	104.3	2.90
65	16.4	56.9	138.3	2.43
65	17.6	43.2	147.6	3.42
66	17.8	32.8	104.1	3.17
85	24.8	45.1	154.3	3.42
86	24.8	75	195.2	2.60
92	29.6	51.4	171.8	3.34
93	28.6	60.3	174.5	2.89
120	57.5	63.4	204.3	3.22
121	55.0	63	205.5	3.26
123	47.6	131	234	1.79
150	62.9	90.9	263.7	2.90
150	75.4	86	264.1	3.07
152	72.1	133.4	235.2	1.76
158	78.7	124.2	299.3	2.41
178	87.3	97.9	262.7	2.68
180	83.8	114.7	272.8	2.38
182	79.5	170.3	295.5	1.74
183	90.0	130.6	306.2	2.34
226	97.1	150.4	364.9	2.43
240	97.0	124.1	313.1	2.52
240	95.7	185.8	319.2	1.72
240	94.7	161.9	344.5	2.13

Fig. 5 Sigmoidal model predictions of conversion of MMA as a function of reaction time for various AIBN concentrations. Lines represent model output data, while spheres represent data obtained using the cylinder system. Model fitting variables: $t_0 = 1800\ s$, $k' = 2.85 * 10^{-3}\ s^{-1}$

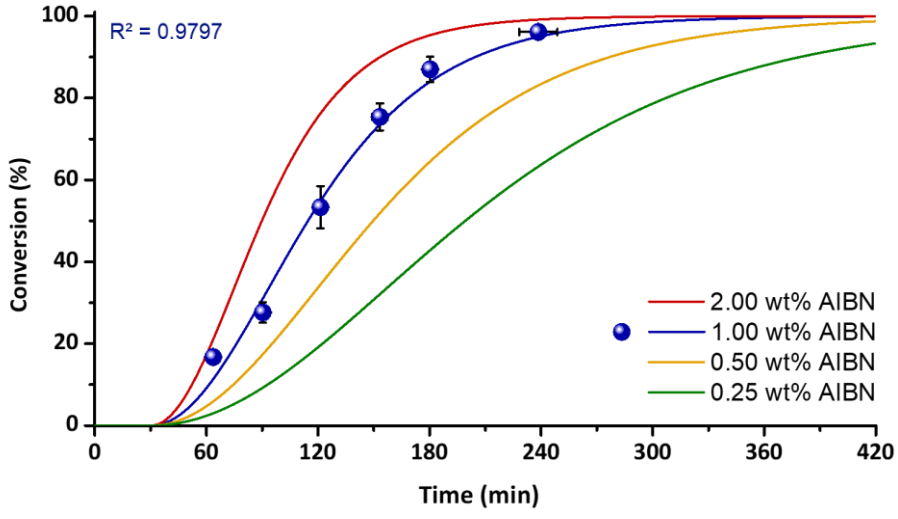

Table 4 Data obtained from samples of polymerisation reactions monitored using the cylinder system. Reaction conditions: 10 ml of MMA, 0.468 g of PDMS-MA, 23.4-187.2 mg of AIBN, 220 bar and 65 ℃
a – determined via ^{1}H NMR, b – determined via GPC

AIBN (wt% wrt MMA)	Reaction time (min)	Conversion (%)[a]	M_n (kDa)[b]	M_w (kDa)[b]	Đ[b]
0.25	91	14.04	201.7	351.4	1.74
0.25	131	18.26	334.5	571.9	1.71
0.25	170	31.03	440.3	718.9	1.63
0.25	202	48.01	482.7	756.5	1.57
0.25	281	64.16	527.6	863.5	1.64
0.25	340	87.73	495.4	791.9	1.60
0.25	400	94.07	518.8	846.5	1.63
0.5	65	12.5	9.3	63.1	6.78
0.5	97	22.7	37	219.7	5.94
0.5	123	29.7	70.7	324.1	4.58
0.5	155	51.2	248.1	429.2	1.73
0.5	188	66.7	297.2	494.6	1.66
0.5	243	89.1	285.8	487.2	1.70
0.5	275	95.4	300.5	550.4	1.83
2	75	28.6	46	99.8	2.17
2	101	49.7	64.6	150.2	2.33
2	118	68.9	84.8	149.7	1.77
2	137	81.3	123.3	193.3	1.57
2	155	90.0	102.9	175	1.70
2	205	94.9	134.7	206.7	1.53
2	300	96.7	114.3	172.8	1.51

Table 5 Data obtained from samples of polymerisation reactions monitored using the cylinder system. Reaction conditions: 10 g of MMA, 0.468 g of PDMS-MA, 23.4-187.2 mg of AIBN, 220 bar and 65 ℃
a – determined via ^{1}H NMR, b – calculated from CPDT and monomer concentration using $M_{n,th} = \left(\frac{[MMA]}{[CPDT]} * conversion\right) * M_{MMA} + M_{CPDT}$, c – determined via GPC

Reaction time (h)	Conversion (%)[a]	$M_{n,th}$ (kDa)[b]	M_n (kDa)[c]	Đ[c]
2	5.66	3.33	4.8	1.16
3	7.41	4.35	5.9	1.19
5.1	14.53	8.54	8.0	1.20
6.1	21.26	12.49	10.5	1.21
8	41.18	24.19	16.2	1.16
10	55.95	32.87	23.5	1.28
24	97.80	57.46	57.3	1.20